Available online at www.sciencedirect.com
SCIENCE DIRECT®
Journal of Sound and Vibration 269 (2004) 455–466
JOURNAL OF SOUND AND VIBRATION
www.elsevier.com/locate/jsvi

Load-response determination for imperfect column using vibratory data

Cheer Germ Go[a,*], Cheng Dar Liou[b]

[a] Department of Civil Engineering, National Chung Hsing University, Taichung, Taiwan 40227, ROC
[b] Department of Civil Engineering, Chien Kuo Institute of Technology, Changhua, Taiwan, ROC

Received 29 April 2002; accepted 20 December 2002

Abstract

In addition to the initial crook to a column, the structural integrity is often not as reliable as expected due to the immaturity of current engineering techniques. Thus, the actual load response is sometimes not consistent with the design predictions for the column. For design considerations, it is necessary to establish experimentally an analytical method for determining the load-deflection curves and buckling load. In this paper, a dynamic method is described for building the load-deflection curves up to its buckling load for an imperfect column. The proposed method does not require the application of axial load and is feasible for arbitrary types of boundary conditions. The load-deflection curves and buckling load are determined from the measured natural frequencies and the vibration modes.

1. Introduction

The columns in engineering structures are functioned to take axial loads. If the axial load is small, the column remains straight and exhibits only axial deformation. At this state, the column is in stable equilibrium. As the magnitude of the load increases to a certain amount, the stable equilibrium becomes unstable and a marked displacement takes place with additional disturbing forces introduced. That is, with the exception of axial deformations, very large lateral displacements are introduced rapidly and eventually lead to failure. In reality, columns are rarely perfectly straight. Owing to various kinds of imperfections, such as initial crookedness, eccentricity in load application, material inhomogeneity, and boundary condition management,

*Corresponding author. Fax: 4-22857-418.
E-mail address: go@mail.ce.nchu.edu.tw (C.G. Go).

0022-460X/03/$ - see front matter
doi:10.1016/S0022-460X(02)01641-3

actual columns behave quite differently under loads from straight columns [1]. Such imperfections may lead to a drastic reduction of the load-carrying capacity of a structure because of the extra moment due to $p-\Delta$ effect [2]. Thus this consideration is included in design manual for practical use. As an example of Structural Stability Research Council column curves were developed by assuming an initial out-of straightness at midheight equal to 0.1% of column length [1]. In addition, the assembly of the structural components is often not as perfect as expected, due to the immaturity of current engineering techniques. The management of boundary conditions is, therefore, not as ideal as design requirement. The existence of such imperfections influences the characteristics of the load-deflection curves predicted in the design. This leads to a considerable difficulty in safety factor selection. The establishment of an experimental method for tracing the load-deflection curves up to its buckling load to guarantee the safety of a structure is necessary. Research efforts [3–11] have been made in the field of buckling load determination. However, the researches on the load-deflection curves prior to a buckling load require comprehensive development. Although the load response may be determined using column deflection measurement, while increasing the imposed axial loads, it may not be feasible to impose the axial load experimentally in most cases. Therefore, an alternative method without imposing axial loads must be developed. In this study, Go's proposal [12–13] was extended for determining the load-deflection curves up to its buckling load for initial crookedness member. This approach requires the excitation of the member. The load response is then determined from the vibratory data, natural frequencies and mode shapes. The proposed approach is suitable for all kinds of boundary conditions and there is no axial force required in the testing process.

2. Analysis model

For a member with an initial crookedness, as shown in Fig. 1, the assumptions are made as follows:

1. The member material is isotropic and linear-elastic.
2. The plane sections remain plane after bending (Kirchhoff's condition).
3. The cross-sectional distortion and shear deformations are relatively small and ignored.
4. The member has a prismatic cross-section uniformly.

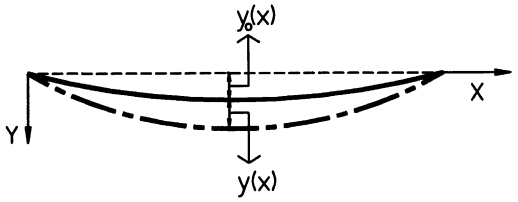

Fig. 1. Scheme for column deflection.

The initial crookedness $y_0(x)$ and deformed shape $y(x)$ induced by axial load may be expressed using Lagrange's interpolation function [14–15],

$$y_0(x) = \sum_{i=1}^{n} N_i(x) d_i, \tag{1}$$

$$y(x) = \sum_{i=1}^{n} N_i(x) D_i, \tag{2}$$

where

$$N_i(x) = \frac{(x - x_1)(x - x_2)\cdots(x - x_{i-1})(x - x_{i+1})\cdots(x - x_n)}{(x_i - x_1)(x_i - x_2)\cdots(x_i - x_{i-1})(x_i - x_{i+1})\cdots(x_i - x_n)} \tag{3}$$

d_i denotes the initial crookedness at the interpolation point x_i, and D_i denotes the deflection induced by the compressive axial load at the interpolation point x_i.

Under the axial load action, the member deforms laterally, as shown in Fig. 2. The axial displacement Δ due to bending caused by the compressive axial load is

$$\begin{aligned} \Delta &= \frac{1}{2}\int_0^l [(y' + y_0')^2 - (y_0')^2]\,\mathrm{d}x \\ &= \frac{1}{2}\int_0^l [(y')^2 + 2(y'y_0')]\,\mathrm{d}x. \end{aligned} \tag{4}$$

The work performed by the applied axial load p is

$$U = p \cdot \Delta = \frac{P}{2}\int_0^l [(y')^2 + 2(y'y_0')]\,\mathrm{d}x. \tag{5}$$

From Eqs. (1) and (2)

$$y'(x) = \sum_{i=1}^{n} N_i'(x) D_i, \quad y_0'(x) = \sum_{i=1}^{n} N_i'(x) d_i. \tag{6}$$

Then

$$U = \frac{P}{2}\int_0^l \left\{\sum_{k=1}^{n} N_k'(x) D_k\right\}^2 \mathrm{d}x + P\int_0^l \left\{\sum_{k=1}^{n}\sum_{j=1}^{n} N_k'(x) N_j'(x) D_k d_j\right\} \mathrm{d}x. \tag{7}$$

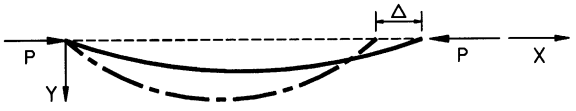

Fig. 2. End displacement of a bend column.

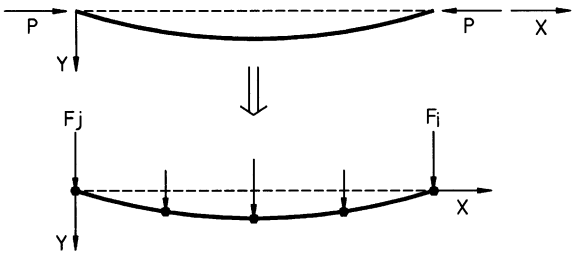

Fig. 3. Scheme for equivalent nodal forces.

The equivalent force F_i, as shown in Fig. 3, corresponding to the deflection in the ith node may be obtained using Castigliano's first theorem as [16]

$$Fi = \frac{\partial U}{\partial D_i} = P\sum_{k=1}^{n}\left\{\int_0^l N_k'(x)N_i'(x)\,\mathrm{d}x\right\}D_k + P\int_0^l\left\{\sum_{j=1}^{n} N_i'(x)N_i'(x)d_j\right\}\mathrm{d}x. \tag{8}$$

Eq. (8) may be represented in matrix form as

$$[F] = P[B][D] + P[Q], \tag{9}$$

where

$$B_{ij} = \int_0^l N_i'(x)N_j'(x)\,\mathrm{d}x, \tag{10}$$

$$Q_i = \int_0^l\left\{\sum_{j=1}^{n} N_i'(x)N_j'(x)d_j\right\}\mathrm{d}x. \tag{11}$$

Also, the equivalent force F_i, may be related to the deflection D_i using

$$[D] = [G][F], \tag{12}$$

where $[G]$ is called the flexibility matrix and its elements G_{ij} are called flexibility influence coefficients. G_{ij} is defined as the displacement at node i due to a unit load applied at node j. Substituting Eq. (9) into Eq. (12) yields

$$[D] = P[G][B][D] + P[G][Q]. \tag{13}$$

Assuming $\lambda = 1/P$ leads to

$$\lambda[D] = [G][B][D] + [G][Q]. \tag{14}$$

Then

$$[D] = \{\lambda[I] - [G][B]\}^{-1}[G][Q], \tag{15}$$

where $[D]$ is the node deflection subjected to axial load p. For $|\lambda[I] - [G][B]| = 0$, the maximum eigenvalue λ_{max} is related to the smallest buckling load P_{cr} using

$$P_{cr} = \frac{1}{\lambda_{max}}. \tag{16}$$

3. Flexibility matrix

The differential equation of free vibration for a structural member may be stated as

$$\frac{d^2}{dx^2}\left\{EI\frac{d^2y(x,t)}{dx^2}\right\} + m\frac{d^2y(x,t)}{dt^2} = 0. \tag{17}$$

Assuming that the solution of Eq. (17) is separable into time and space factors, one may write

$$y(x,t) = \sum_{k=1}^{\infty} \phi_k(x)T_k(t). \tag{18}$$

Substituting Eq. (18) into Eq. (17) leads to two ordinary differential equations

$$\frac{d^2}{dx^2}\left(EI\frac{d^2\phi_k(x)}{dx^2}\right) - m\omega_k^2\phi_k(x) = 0, \tag{19}$$

$$\frac{d^2T_k(t)}{dt^2} + \omega_k^2 T_k(t) = 0, \tag{20}$$

where ω_k and $\phi_k(x)$ are the natural frequency and the corresponding modal shape of the kth mode respectively. The modal shape, $\phi_k(x)$ must satisfy the orthogonality condition

$$\sum_{i=1}^{\infty}\int_0^l m\phi_i(x)\phi_j(x)dx = M_i\delta_{ij}, \tag{21}$$

where δ_{ij} is the Kronecker delta.

The equivalent equation for the aforementioned system which is subjected to a static unit load $F = \delta(x-\eta)$, at the position $x = \eta$, may be expressed as

$$\frac{d^2}{dx^2}\left\{EI\frac{d^2y(x)}{dx^2}\right\} = \delta(x-\eta), \tag{22}$$

where

$$\int_0^l \delta(x-\eta)\,dx = \begin{cases} 1 & x = \eta \\ 0 & x \neq \eta. \end{cases} \tag{23}$$

By Galerkin's method, $y(x)$ may be approximated by a linear combination of function $(\phi_1, \phi_2, \phi_3, \ldots)$ as

$$y(x) = \sum_{k=1}^{\infty} a_k\phi_k(x), \tag{24}$$

where a_k are constants to be determined. Therefore,

$$\sum_{k=1}^{\infty} a_k \int_0^l \frac{\mathrm{d}^2}{\mathrm{d}x^2}\left\{ EI \frac{\mathrm{d}^2\phi_k(x)}{\mathrm{d}x^2} \right\} \phi_i(x)\,\mathrm{d}x = \int_0^l \delta(x-\eta)\phi_i(x)\,\mathrm{d}x. \tag{25}$$

By comparing Eq. (19) with Eq. (25), the unknown constants a_k may be simplified by using Eq. (21) as

$$a_i = \frac{\phi_i(\eta)}{M_i\omega_i^2}. \tag{26}$$

The deflection curve $y(x)$ may thus be obtained by substituting Eq. (26) into Eq. (24), to yield

$$y(x) = \sum_{k=1}^{\infty} \frac{\phi_k(\eta)\phi_k(x)}{M_k\omega_k^2}. \tag{27}$$

For $\eta = x_i$, the flexibility influence coefficient G_{ij} in Eq. (12) can then be determined as [17]

$$G_{ij} = y(x_i) = \sum_{k=1}^{\infty} \frac{\phi_k(x_i)\phi_k(x_j)}{M_k\omega_k^2}. \tag{28}$$

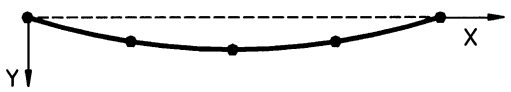

Fig. 4. Uniform distribution of 5 stations.

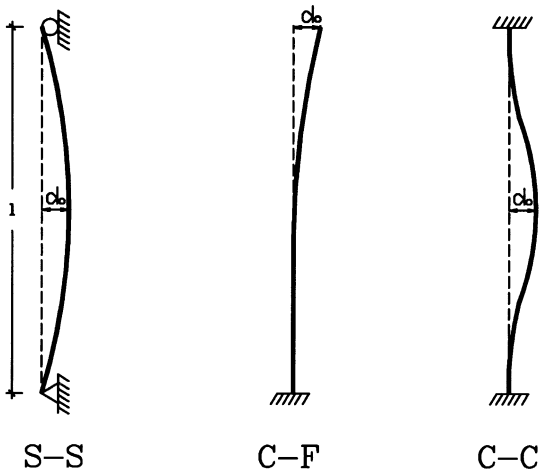

Fig. 5. Example column for analysis on solution consideration.

All of the information regarding the boundary conditions and material properties are contained implicitly in this parameter G_{ij} [9].

4. Solution consideration

Theoretically, the interpolation function of Eqs. (1) and (2) for the initial crookedness and deformed shape plays a dominating role in the accuracy. Proper selection of the interpolation points (i.e., stations in the experimentation) may lead to a well-defined shape and result in a satisfactory solution, as shown in Fig. 4. Three examples with extreme end constraints (i.e., free end and clamped end constraints) were chosen to illustrate the feasibility of this method. As shown in Fig. 5, the S, C, and F represent simply supported, clamped and free ends, respectively. In reality, the initial crookedness is arbitrarily random. Nevertheless, the crook magnitude up to 0.5% of the member length is used in calculation for comparisons with theoretical results. These examples are performed as follows:

Case 1: is a simply supported column with initial crookedness $y_0(x)$, $y_0(x) = d_0 \sin(\pi x/l)$.
Case 2: is a clamped–free column with initial crookedness $y_0(x)$, $y_0(x) = d_0 : (1 - \cos(\pi x/2l))$.
Case 3: is a clamped–clamped column with initial crookedness $y_0(x), y_0(x) = d_0\left(\frac{1}{2} - \frac{1}{2}\cos(2\pi x/l)\right)$.

By referring to Eqs. (3) and (17), five stations were selected for the example, as shown in Fig. 4. The finite element method (FEM) solutions for the free vibration of the example were utilized to establish the flexibility matrix. These were required for establishing the load-deflection curves. Vibratory parameters of the first five modes were used. The initial crookedness of the example member at the test station is shown in Table 1. The subject load-deflection curves are shown in Figs. 6–8. These results for the initial crookedness members with end conditions such as S–S, C–F are in very good agreement with the theoretical solutions except for case C–C. The main reason for this disagreement may be that the chosen function does not represent properly the structural member deflection for the case C–C. Theoretically, the distance between the structural member inflection points, i.e., the effective length, significantly affects the buckling load. In other words, this effective length may significantly influence the accuracy of interpolation function for describing the column deflection. Thus an increasing number of test stations, providing a better representation of the deformed shape, may improve the results. This improvement is shown in Fig. 8 for 7 stations instead of 5 stations. For the case C–C, 7 stations were implemented, the load-deflection curves is very close to the theoretical solution. All of these examples lead to the conclusion that the 7 stations arrangement is sufficient for dependable accuracy.

Table 1
Initial crookedness at the test station

	1	2	3	4	5
S–S	0	$0.707d_0$	d_0	$0.707d_0$	0
C–F	0	$0.076d_0$	$0.293d_0$	$0.617d_0$	d_0
C–C	0	$0.5d_0$	d_0	$0.5d_0$	0

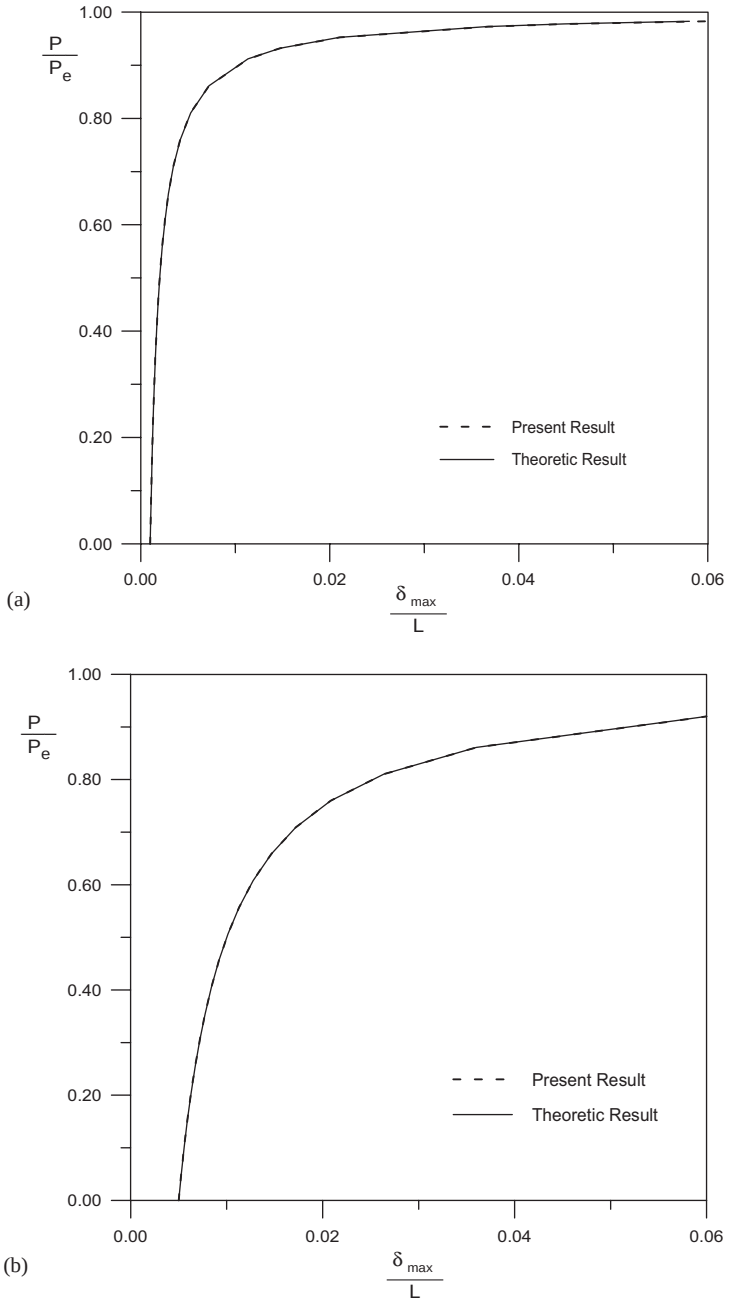

Fig. 6. Load-deflection curve of S–S column for five stations (a) $d_0 = 0.001l$, (b) $d_0 = 0.005l$.

5. Feasibility of experimental identification

In practice, the accuracy of the experimental determination of load-deflection curves is always affected by factors such as experimental apparatus error, operator error, etc. To assess the

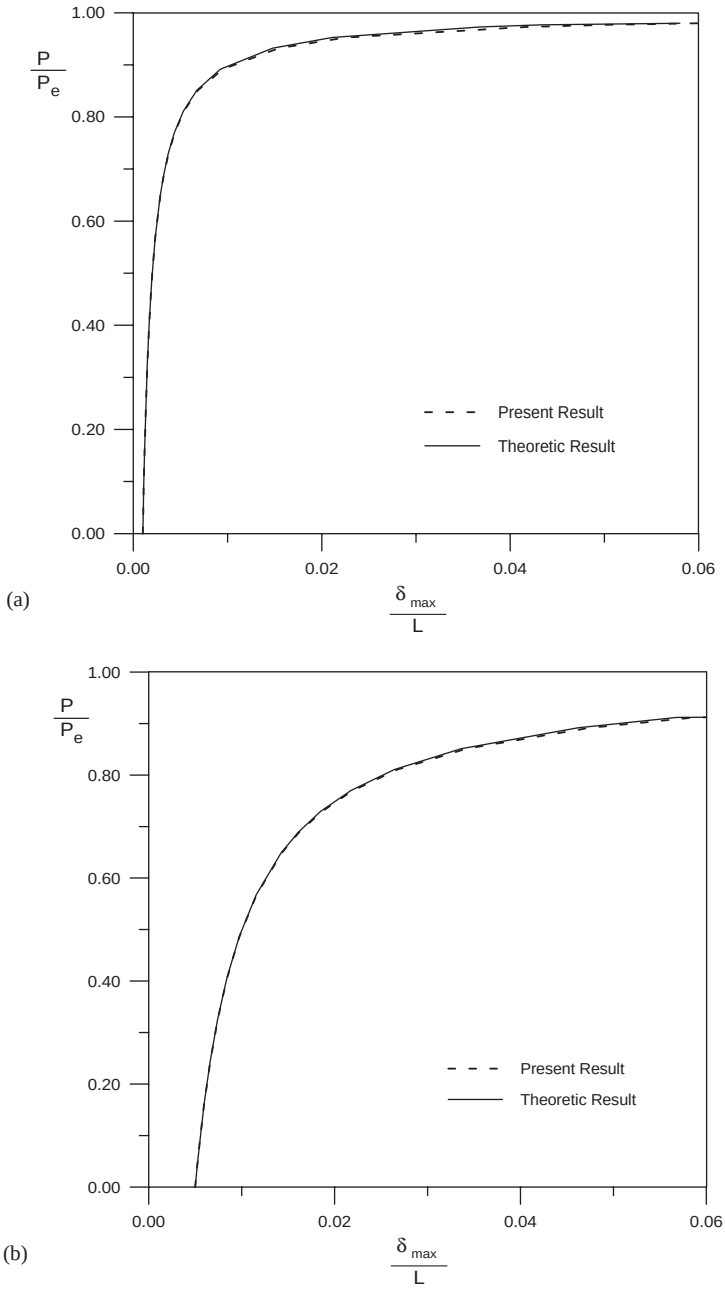

Fig. 7. Load-deflection curve of C–F column for five stations (a) $d_0 = 0.001l$ (b) $d_0 = 0.005l$.

possible errors for load-deflection curves determination, a simulation experiment was designed [18] and carried out as follows:

(1) Calculation of theoretical vibration parameters $[\bar{\phi}_n]$ and $\bar{\omega}_n$;

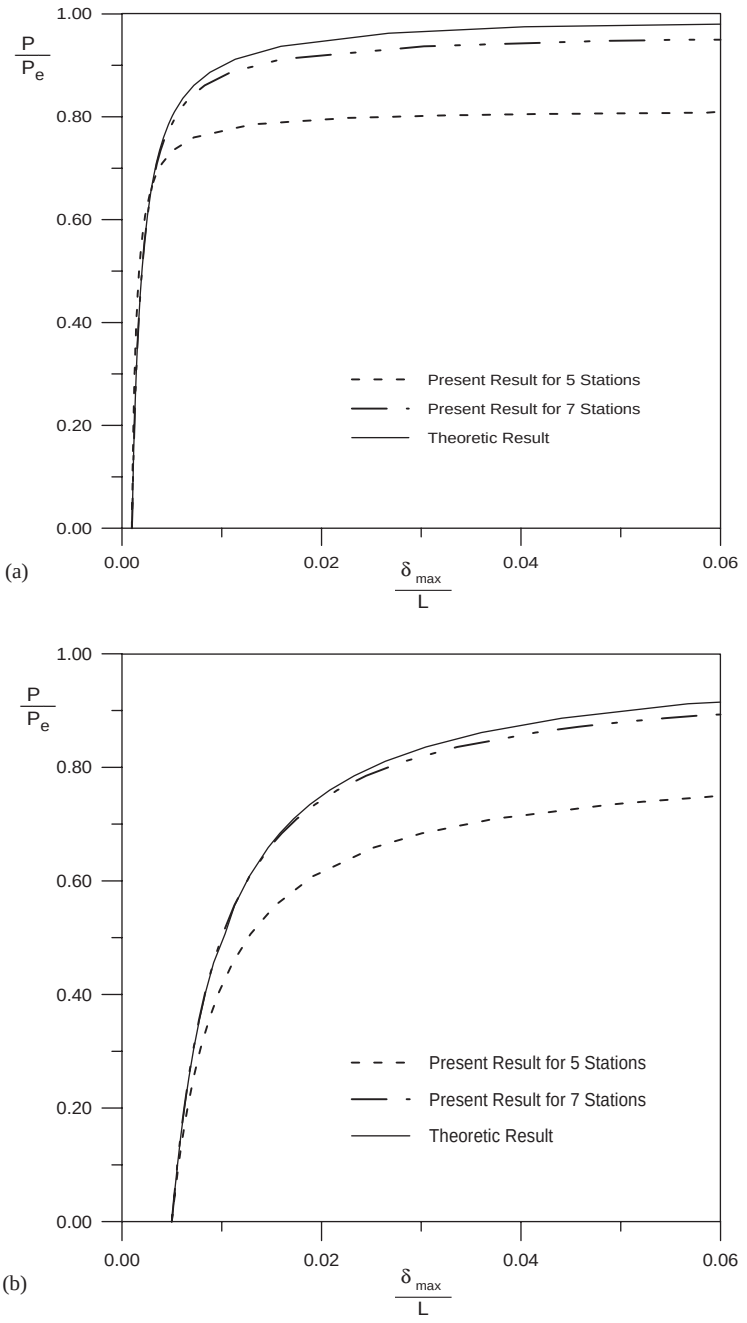

Fig. 8. Load-deflection curve of C–C column (a) $d_0 = 0.001l$, (b) $d_0 = 0.005l$.

(2) generation of experimental errors e within an error range e_r using the Monte-Carlo method [18], where $e = e_r \times RAN_u$ and RAN_u is a normal distribution random number between –1 and 1;

Table 2
Maximum deviation % errors of simulation experiments

Experimental error range (%)	Boundary condition		
	S–S	C–F	C–C
2	5	8	8
4	10	14	14
6	15	20	20

(3) simulation of experimental vibration parameters $[\phi_n]$ and ω_n using formulas $\phi_i = \bar{\phi}_i \times (1 + e_i)$ and $\omega_n = \bar{\omega}_n \times (1 + e_n)$;
(4) determination of $[G]$ using Eq. (28);
(5) determination of $[B]$ using Eq. (10);
(6) establishment of the load-deflection curves using Eq. (15).

In this analysis, three different cases, with error ranges, 2%, 4% and 6% were taken into consideration. With 10,000 simulation experiments in each case, the load-deflection curves deviating from the theoretical curve are shown in Table 2. It may be inferred that the accuracy of the load-deflection curves identification is proportional to the measurement errors.

Since the model testing technique is well established, an identification error within 3% can easily be reached. This means, from Table 2, that the proposed approach can provide an effective way to establish the load-deflection curves.

6. Conclusions

An analysis model for the load-deflection curves up to its buckling load for an initial crookedness member was proposed. The main advantages of applying the proposed approach may be stated as follows:

(1) Only dynamic parameters are required, i.e., natural frequencies and the corresponding mode shapes, for load-deflection curves determination.
(2) The satisfied result is available regardless of the kind of boundary conditions.
(3) There is no axial force required in the process.
(4) The material properties are not required in the process of load-deflection curves determination.

References

[1] E.M. Lui, W.F. Chen, Simplified approach to the analysis and design of columns with imperfections, AISC Engineering Journal 21 (1984) 99–117.
[2] I. Elishakoff, Y. Li, J.H. Starnes, Non-Classical Problems in Theory of Elastic Stability, Cambridge University Press, Cambridge, 2001.
[3] R. Lurie, Lateral vibration as related to structural stability, Journal of Applied Mechanics 19 (1952) 195–203.

[4] M. Baruch, Integral equations for nondestructive determination of buckling loads for elastic plate and bars, Israel Journal of Technology 11 (1973) 1–8.
[5] A.L. Sweet, J. Genin, Identification of a model for predicting elastic buckling, Journal of Sound and Vibration 14 (1971) 317–324.
[6] A.L. Sweet, J. Genin, P.F. Mlakar, Vibratory identification of beam boundary conditions, Journal of Dynamic Systems, Measurement and Control 98 (4) (1976) 387–394.
[7] A.L. Sweet, J. Genin, P.F. Makar, Determination of column buckling criteria using vibratory data, Experimental Mechanics 117 (1977) 385–391.
[8] A. Segall, G.S. Springer, A nondestructive dynamic method for determination of the critical load of elastic column, Experimental Mechanics 20 (1980) 285–288.
[9] A. Segall, G.S. Springer, A dynamic method for measuring the critical loads of elastic flat plate, Experimental Mechanics 26 (1986) 354–359.
[10] P.A.A. Laura, R.E. Rossi, On the relative accuracy and relative difficulties of vibrations and buckling problems of structural elements, Journal of Sound and Vibration 134 (3) (1989) 381–387.
[11] C.H. Yoo, J.K. Young, J.S. Davidson, Buckling analysis of curved beam-columns by finite-element discretization, American Society of Civil Engineers Journal of Engineering Mechanics 122 (8) (1996) 761–770.
[12] C.G. Go, Y.S. Lin, E.H. Khor, Experimental determination of the buckling load of a straight structural member by using dynamic parameters, Journal of Sound and Vibration 205 (3) (1997) 257–264.
[13] C.G. Go, C.D. Liou, Experimental determination of the buckling load of a flat plate by the use of dynamic parameters, Structural Engineering and Mechanics 9 (5) (2000) 483–490.
[14] O.C. Zienkiewicz, R.L. Taylor, in: The Finite Element Method, Vol. I, McGraw-Hill, London, 1989.
[15] O.C. Zienkiewicz, R.L. Taylor, in: The Finite Element Method, Vol. II, McGraw-Hill, London, 1991.
[16] A. Ghali, A.N. Neville, Structural Analysis, Chapman and Hall, London, 1978.
[17] R.L. Bisplinghoff, H. Ashley, R.L. Halfman, Aeroelasticity, Addison-Wesley, New York, 1955.
[18] F.S. Hillier, Q.J. Liberman, Operations Research, Hoden-Day, San Francisco, 1974.